Induction of Relaxor Behavior in $Na_{1-x}Sr_{x/2}\square_{x/2}NbO_3$ through the Introduction of Cationic Vacancies

Almudena Torres-Pardo,[†] Ricardo Jiménez,[‡] Jose M. González-Calbet,[†] and Ester García-González*,[†]

Departamento de Química Inorgánica, Facultad de Químicas, Universidad Complutense Madrid, Madrid 28040, Spain and Instituto de Ciencia de Materiales de Madrid, CSIC Cantoblanco, Madrid 28049, Spain

Received January 12, 2009. Revised Manuscript Received March 5, 2009

Materials in the $Na_{1-x}Sr_{x/2}\square_{x/2}NbO_3$ system ($0.3 \leq x \leq 0.4$) have been investigated by combining diffraction methods and high resolution electron microscopy with dielectric measurements. They undergo a microstructural evolution by continuously decreasing the coherent structural domain size as a consequence of the random distribution of the growing A-vacancy concentration. Change in the electrical properties occurs from the achievement of relaxor ferroelectric character in $Na_{0.7}Sr_{0.15}NbO_3$ to the strongly diffuse phase transition of $Na_{0.6}Sr_{0.2}NbO_3$. The nanometric size of the structural domains found in the relaxor material led us to discuss the relationship between structural domain and polar region.

Introduction

Relaxor ferroelectrics include a large group of random lattice disorder ABO_3 perovskites. Much of this disorder is produced by chemical substitution of ions of the same or different oxidation state of the host. In addition to being an essential feature, lattice disorder is at the origin of local polar clusters of randomly oriented polarization,[1−4] the so-called polar nanoregions (PNRs), that appear at temperatures far above the temperature of the maximum dielectric permittivity (Burns temperature). On cooling, the PNRs evolve changing their dynamics and producing a slowing down of the dielectric relaxation that is associated with the large and wide frequency dispersion peak in the temperature dependence of the dielectric constant. On further cooling, the PNRs can become frozen in a cooperative state that in some cases can produce a ferroelectric long-range order. The dielectric peak observed in relaxors is usually of the same order of magnitude as the peaks at the Curie point in the ordinary ferroelectric perovskites, but in contrast to common ferroelectrics it is highly diffuse and it does not account for a structural phase transition.[5−7] The interest in understanding the physical mechanism responsible for diffuse phase transitions, as well as their excellent piezoelectric response which qualifies them for potential applications, is the two main reasons underlying the great amount of studies focused on relaxor ferroelectric materials in the last years.[8,9] Although most of the work developed in this area has been devoted to lead containing materials derived from the perovskite structure,[10,11] environmental requirements have led to propelling the search for lead-free ABO_3 compounds with ferroelectric character. In this sense, diverse materials deriving from $BaTiO_3$ have shown interesting properties in strong competition with the best lead-containing relaxors.[12−14] Sodium niobate is the last candidate considered to obtain materials with dielectric properties for potential applications. Although $NaNbO_3$ is an antiferroelectric material at room temperature, ferroelectricity can be induced by adequately modifying the chemical composition.[15,16] Most of the studies devoted to $NaNbO_3$-derived materials focus on the preparation of new compounds with relaxor-type behavior.[17,18] In this sense, relaxor ferroelectric materials have been found in the $NaNbO_3-Na_{0.5}Bi_{0.5}TiO_3$ and $NaNbO_3-Sr_{0.5}NbO_3$ systems.[19] In the case of the strontium doped solid solution,

* Corresponding author. Tel.: +34-913944518. Fax: +34-913944352. E-mail: esterg@quim.ucm.es.
† Universidad Complutense Madrid.
‡ CSIC Cantoblanco.

(1) Keemann, W. *J. Mater. Sci.* **2006**, *41*, 129–136.
(2) Xu, G.; Gehring, P. M.; Shirane, G. *Phys. Rev. B* **2006**, *74*, 104110.
(3) Liu, Y.; Withers, R. L.; Nguyen, B.; Elliott, K. *Appl. Phys. Lett.* **2007**, *91*, 152907.
(4) Xu, G.; Wen, J.; Stock, C.; Gehring, P. M. *Nat. Mater.* **2008**, *7*, 562–566.
(5) Cross, L. E. *Ferroelectrics* **1987**, *76*, 241–267.
(6) Samara, G. A. *J. Phys.: Condens. Mater* **2003**, *15*, R367−R411.
(7) Bokov, A. A.; Ye, Z.-G. *J. Mater. Sci.* **2006**, *41*, 31–52.
(8) Xu, G.; Zhong, Z.; Bing, Y.; Ye, Z.-G.; Shirane, G. *Nat. Mater.* **2006**, *2*, 134–140.
(9) Mani, R.; Achary, S. N.; Chakraborty, K. R.; Deshpande, S. K.; Joy, J. E.; Nag, A.; Gopalakrishnan, J.; Tyagi, A. K. *Adv. Mater.* **2008**, *20*, 1348–1352.
(10) Lente, M. H.; Moreira, E. N.; Garcia, D.; Eiras, J. A.; Neves, P. P.; Doriguetto, A. C.; Mastelaro, V. R.; Mascarenhas, Y. P. *Phys. Rev. B* **2006**, *73*, 054106.
(11) Long, X.; Ye, Z.-G. *J. Appl. Phys.* **2007**, *101*, 124101.
(12) Khemakhem, H.; Simon, A.; Von Der Mühll, R.; Ravez, J. *J. Phys.: Condens. Matter* **2000**, *12*, 5951–5960.
(13) Lu, S. G.; Xu, Z. K.; Chen, H. *Appl. Phys. Lett.* **2004**, *85*, 5319.
(14) Yu, H.; Ye, Z.-G. *J. Appl. Phys.* **2008**, *103*, 034114.
(15) Ivliev, M. P.; Raevskii, I. P.; Reznichenko, L. A.; Raevskaya, S. I.; Sakhnenko, V. P. *Phys. Solid State* **2003**, *45*, 1984–1989.
(16) Jiménez, R.; Sanjuán, M. L.; Jiménez, B. *J. Phys.: Condens. Matter* **2004**, *16*, 7493–7510.
(17) Raevski, I. P.; Prosandeev, S. A. *J. Phys. Chem. Solids* **2002**, *63*, 1939–1950.
(18) Raevski, I. P.; Reznitchenko, L. A.; Malitskaya, M. A.; Shilkina, L. A.; Lisitsina, S. O.; Raevskaya, S. I.; Kuznetsova, E. M. *Ferroelectrics* **2004**, *299*, 95–101.
(19) Raevskaya, S. I.; Reznitchenko, L. A.; Raevski, I. P.; Titov, V. V.; Titov, S. V.; Dellis, J.-L. *Ferroelectrics* **2006**, *340*, 107–112.

10.1021/cm9000834 CCC: $40.75
Published on Web 04/23/2009

$Na_{1-x}Sr_{x/2}\square_{x/2}NbO_3$, the Nb(V) concentration is preserved by introducing a variable amount of A-vacancies (□ denotes A-vacancy). The progressive stabilization of a ferroelectric material occurs for the $x = 0.2$ composition through the random accommodation of a continuously increasing A-vacancy concentration.[20]

New interest arises in the study of the $Na_{1-x}Sr_{x/2}\square_{x/2}NbO_3$ system from the change in the electric properties observed for compositions above $x = 0.2$. In the present contribution, we study the evolution suffered by this system as dopant and, therefore, A-vacancy content increases, obtaining relaxor properties for the $x = 0.3$ composition and strongly diffuse phase transition for $x = 0.4$ which is the limit of the solid solution. The influence of A-vacancies creation on the dielectric properties is not a well studied phenomenon and only a small number of examples have been reported in the literature, [21−24] but a simultaneous study of the structural and microstructural evolution through the doping process and the relationship with the observed dielectric properties has not yet been reported.

We present in this work the results obtained by combining diffraction methods and high resolution electron microscopy with dielectric measurements in the characterization of the evolution of the $Na_{1-x}Sr_{x/2}\square_{x/2}NbO_3$ system. The modification of the dielectric properties is interpreted on the basis of a gradual increment of randomly distributed A-vacancy positions as a consequence of the doping process.

Experimental Section

Samples with nominal composition $Na_{1-x}Sr_{x/2}\square_{x/2}NbO_3$ ($0.2 \leq x \leq 0.4$) were prepared by the conventional ceramic technique. Corresponding stoichiometric amounts of $SrCO_3$ (99.9%, Merck), Na_2CO_3 (99.5%, Merck), and Nb_2O_5 (99.99%, Aldrich) were mixed in an agate mortar and heated in platinum crucibles at 1173 K for 12 h to decompose the different carbonates. The resulting powders were reground in an agate mortar, pelleted, and heated in air at 1473 K. Samples were finally cooled to room temperature at a cooling rate of 1.5 K min^{-1}.

The average cationic compositions of the samples were determined on a JEOL 8900 "Super Probe" electron probe microanalyzer with five wavelength-dispersive spectrometers (WDS) operating at 20 kV and 50 μA. Average cationic composition of all the samples was confirmed as the nominal composition.

Room temperature powder X-ray diffraction (XRD) patterns for all samples were collected on a Panalytical X'PERT PRO ALPHA 1 diffractometer with a Ge(111) primary beam monochromator prealigned for Cu Kα_1 radiation and provided with a X'Celerator fast detector. High temperature powder XRD data in air were measured on a Panalytical X'PERT PRO θ θ-diffractometer supplied with a X'Celerator fast detector and Ni β-filter with Cu Kα radiation. Effective step time of 800 s and a step size of 0.017 and 0.033 (deg/2θ) were used to record data for Rietveld analysis[25] at room and high temperature, respectively.

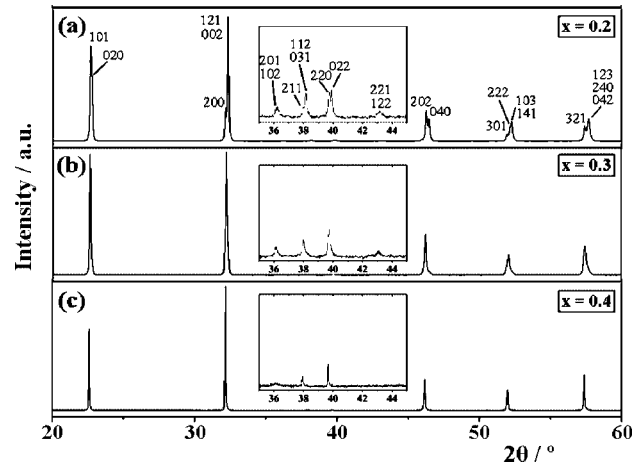

Figure 1. Room temperature powder XRD patterns corresponding to the (a) $x = 0.2$, (b) $x = 0.3$, and (c) $x = 0.4$ compositions of the $Na_{1-x}Sr_{x/2}\square_{x/2}NbO_3$ system. Miller indices are referred to the $\sqrt{2}a_c \times 2a_c \times \sqrt{2}a_c$ unit cell.

Samples for transmission electron microscopy were ultrasonically dispersed in *n*-butanol and transferred to carbon coated copper grids. Selected area electron diffraction (SAED) experiments were carried out on a PHILIPS CM20FEG SuperTwin electron microscope. High resolution electron microscopy (HREM) was performed on a JEOL JEM300FEG electron microscope.

Dielectric properties were measured on a HP 4284A impedance analyzer. Measurements were carried out as a function of temperature (80−750 K) at selected frequencies between 10^2 and 10^6 Hz on disk-shaped specimens of 13 mm diameter and 0.9 mm thickness sintered in air at 1373 K for 24 h (density >98%). Gold paste (Dupont QG 150) sintered at 1123 K was used as an electrode. The polarization electric field ($P-E$) hysteresis loops were obtained by means of the virtual ground technique. High voltage sine waves of 0.1 Hz frequency were applied by the combination of a HP3325B synthesizer/function generator and a bipolar operational power supply/amplifier (TREK 10/40 A), while charge was measured with a home-built charge to voltage converter.

Results

Figure 1 shows the room temperature powder X-ray diffraction (XRD) patterns corresponding to the oxides with composition $Na_{1-x}Sr_{x/2}\square_{x/2}NbO_3$ ($0.2 \leq x \leq 0.4$). Single phase materials with perovskite-type structure were found over the studied composition range. For compositions $x > 0.4$, a small amount of a tetragonal tungsten bronze type-phase was observed as impurity phase.

The XRD pattern for the $x = 0.2$ composition (Figure 1a) could be indexed on the basis of a twofold orthorhombic perovskite superstructure, space group $P2_1ma$ (No. 26) with cell parameters $a \approx c \approx \sqrt{2}a_c$, $b \approx 2a_c$,[20] isostructural with the Q-phase of $NaNbO_3$[26] where subindex c refers to the cubic perovskite. Patterns corresponding to the $x = 0.3$ and

(20) Torres-Pardo, A.; Jiménez, R.; González-Calbet, J. M.; García-González, E. *Chem. Mater.* **2008**, *20*, 6957–6964.
(21) Farhi, R.; El Marssi, M.; Simon, A.; Ravez, J. *Eur. Phys J. B* **2000**, *18*, 605–610.
(22) Mishchuk, D. O.; V'yunov, O. I.; Ovchar, O. V.; Belous, A. G. *Inorg. Mater.* **2004**, *40*, 1324–1330.
(23) Ravez, J.; Simon, A. *Solid State Sci.* **2000**, *2*, 525–529.
(24) Zuo, R.; Su, S.; Wu, Y.; Wang, M.; Li, L. *Mater. Chem. Phys.* **2008**, *110*, 311–315.
(25) Rodríguez-Carvajal, J.; Roisnel, T. *FullProf, WinPLOTR* and accompanying programs; 1999 (http:// www-llb.cea.fr/fullweb/powder.htmf).
(26) Shuvaeva, A.; Antipin, M. Yu.; Lindeman, S. V.; Fesenko, O. E.; Smotrakov, V. G.; Struchkov, Yu. T. *Ferroelectrics* **1993**, *141*, 307–311.

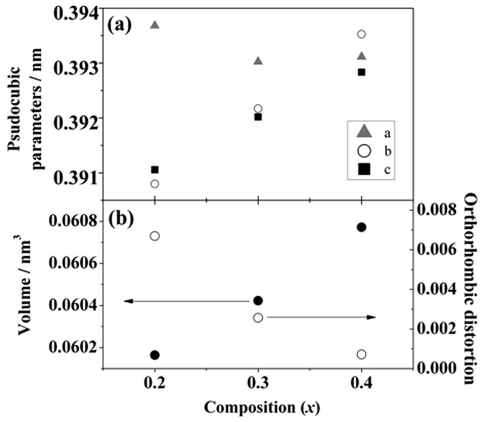

Figure 2. (a) Pseudocubic lattice parameters obtained from the analysis of the room temperature XRD patterns for $Na_{1-x}Sr_{x/2}\square_{x/2}NbO_3$ ($0.2 \leq x \leq 0.4$). (b) Composition dependence of the orthorhombic distortion and unit cell volume.

0.4 compositions (Figure 1b,c, respectively) show the presence of diffraction maxima around 36 and 38°/2θ which led us to index both diffractograms on the basis of an orthorhombically distorted $\sqrt{2}a_c \times 2a_c \times \sqrt{2}a_c$ perovskite-type cell, hereafter referred to as Q-like cell, although their relative intensity becomes very low in the case of the $x = 0.4$ composition. In addition, a significant decrease of the splitting of the diffraction maxima is observed as strontium content increases. Figure 2a shows the pseudocubic lattice parameters for $Na_{1-x}Sr_{x/2}\square_{x/2}NbO_3$ ($0.2 \leq x \leq 0.4$) samples obtained from the analysis of the XRD data. Composition dependence of the orthorhombic distortion, calculated as $2(a - c)/(a + c)$, can be observed, the pseudocubic b and c parameters increasing in a roughly linear way with the increase in the strontium content and the pseudocubic a parameter maintaining its value nearly constant (Figure 2b).

The use of transmission electron microscopy revealed that the creation of a variable amount of A-vacancies by partial substitution of strontium by sodium in the $Na_{1-x}Sr_{x/2}\square_{x/2}NbO_3$ system has an important influence on the structure and, consequently, on the electrical properties of the samples for the $0 < x \leq 0.2$ composition range.[20] Accommodation of the vacancy positions over this composition range occurs through random distribution in the A sublattice of the perovskite cell giving rise to the appearance of a twofold superstructure of sodium niobate, the so-called Q-like phase, for the $x = 0.2$ composition with ferroelectric behavior ($T_c = 448$ K). Crystals of the ferroelectric $Na_{0.8}Sr_{0.1}NbO_3$ material are constituted by structural domains (average size ~100 nm) of a Q-like phase. Since the formation of the $Na_{1-x}Sr_{x/2}\square_{x/2}NbO_3$ solid solution implies the continuous creation of an increasing amount of A vacancies, it is interesting to investigate the microstructural effect when doping the ferroelectric material for compositions $x > 0.2$. The role of the strontium−vacancy pair in the electric properties of the samples could then be easily elucidated when correlating the microstructural characterization of the samples and their electric properties.

Figure 3a corresponds to the SAED pattern of a crystal of $Na_{0.7}Sr_{0.15}NbO_3$. The diffraction pattern can be interpreted as the overlapping of an orthorhombic $\sqrt{2}a_c \times 2a_c \times \sqrt{2}a_c$ unit cell in the [010] and [10$\bar{1}$] reciprocal lattice projections, the last one being oriented in two perpendicular directions. Notice that the forbidden (100) reflection is observed by multiple diffraction. This interpretation is confirmed by the corresponding electron micrograph shown in Figure 3b. Distances of 0.79 and 0.55 nm can be easily measured, but contrast in the image is clearly heterogeneous because structural domains are restricted to a few nanometers. The increasing amount of A-vacancies seems to limit the domain growth to the nanometric scale, giving rise to the characteristic aspect of a short-range ordered situation. As a consequence, diffraction maxima corresponding to the formation of nanodomains appear broad and diffuse in the SAED pattern. No evidence of strontium/sodium/vacancy order is found, so a random distribution of vacancies can be assumed to occur in the A sublattice of the material. Therefore, crystals of $Na_{0.7}Sr_{0.15}NbO_3$ are formed by structural domains of the Q-like phase of around 10 nm size.

Figure 4a displays the temperature dependence of the real part of the relative dielectric constant (K') at different measuring frequencies for the $x = 0.3$ composition. A broad peak of K' around 344 K at 1 kHz is observed. The temperature of the dielectric maximum in K' (T_m) is shifted to higher values as frequency increases, and the frequency dependence of T_m follows the empirical Vogel-Fulcher law[27] (Figure 4b), with a freezing temperature $T_f = 330$ K, activation energy $E_a = 25$ meV, and relaxation frequency ω_0 close to 7×10^{13} rad s^{-1}. A frequency dispersion takes place for $T \leq T_m$, the value of K' decreasing when frequency increases. This behavior indicates a relaxor ferroelectric character for this material.[5,7] Hysteresis loop can be achieved in the polarization versus electric field curve at temperatures below T_f. The P_r and the E_c were 3.69 μC cm^{-2} and 5.6 kV cm^{-1} at 293 K, respectively (Figure 4c). The hysteresis loops measured in the 275−395 K range become slimmer when temperature increases, and at the same time a gradual decrease of the P_r above T_m occurs (Figure 4d) which is consistent with the relaxor ferroelectric behavior observed.[6] The Curie−Weiss fit of $1/K'$ vs T shows paraelectric behavior from 542 K which can be identified as the Burns temperature of the system (Figure 4e).

The electrical characterization performed over the $x = 0.3$ compositions reveals a deviation from the ferroelectric character of $Na_{0.8}Sr_{0.1}NbO_3$ ($x = 0.2$) as a result of increasing the dopant content. As described above, the microstructural study performed by TEM shows that crystals of both materials appear to be constituted by structural domains of the orthorhombically distorted Q-like phase, the most striking difference between them being the average domain size. To understand the correspondence between the presence of the Q-like phase and the polar character in the $x = 0.3$ composition, it would be interesting to analyze the temperature evolution of the structure for the relaxor ferroelectric material as well as for the ferroelectric material from which it is obtained. Comparison between them would help to understand the breaking of the long coherent length of the polar domains.

(27) Viehland, D.; Jang, S. G.; Cross, L. E.; Wutting, M. *J. Appl. Phys.* **1990**, *68*, 2916.

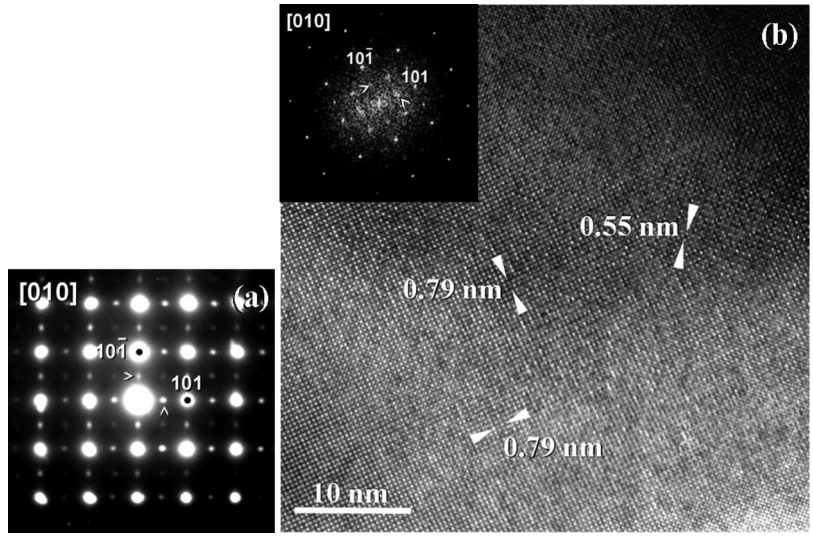

Figure 3. (a) SAED pattern of $Na_{0.7}Sr_{0.15}NbO_3$ taken along [010] zone axis. Arrows show diffraction maxima corresponding to the twofold superstructure oriented in two perpendicular directions. (b) Corresponding high resolution electron micrograph where areas (~10 nm) with the three different perpendicular orientations are observed. Fourier transform is shown as inset.

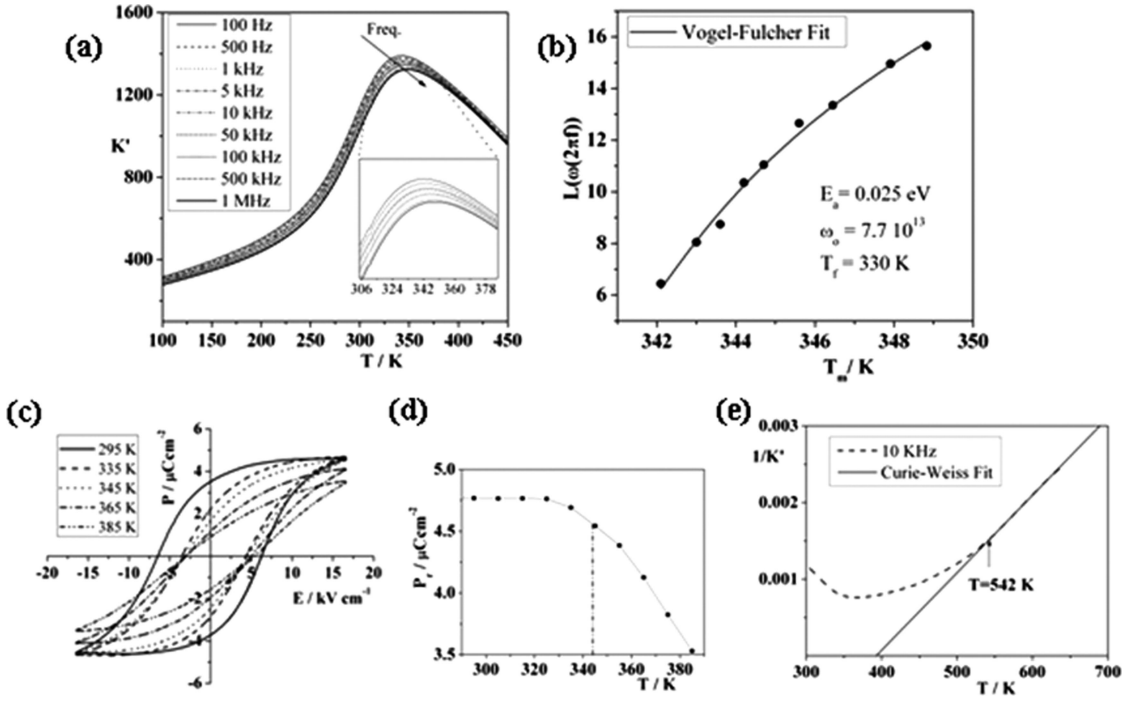

Figure 4. (a) Temperature dependence of K' at different measurement frequencies for $Na_{0.7}Sr_{0.15}NbO_3$. (b) Corresponding frequency dependence of T_m (points) and Vogel-Fulcher curve. (c) Polarization vs electric field at different temperatures for the $Na_{0.7}Sr_{0.15}NbO_3$ material. (d) Remnant polarization as a function of the temperature measured from the $P(E)$ curves. (e) Inverse of K' as a function of the temperature at 10 kHz showing Curie−Weiss fit for $T >$ 542 K.

In this sense, high temperature XRD patterns were collected for both the $x = 0.2$ and the $x = 0.3$ compositions. Measurements were done by collecting data from 298 to 1023 K at intervals of 25 K. Figure 5a,b shows the sequence of patterns recorded as temperature increases in the 35−42°/2θ-range for $x = 0.2$ and $x = 0.3$, respectively. The ferroelectric character of the room temperature $x = 0.2$ material allows its unit cell to be described in the non-centrosymmetric space group $P2_1ma$ (No. 26). The upper part of Figure 5a shows diffraction maxima of the room temperature phase in the 36−38°/2θ range, where the observed splitting is caused by the orthorhombic lattice distortion. The upper part of Figure 5b shows the same diffraction maxima for the room temperature $x = 0.3$ phase, which account for the orthorhombic distortion in respect to the cubic perovskite cell. Provided the lack of information supplied by diffraction methods concerning the presence of the center of symmetry, the relaxor ferroelectric behavior of this material led us to assume that a nonpolar crystal phase should be considered to describe the room temperature phase of the $x = 0.3$ sample. The temperature evolution (middle part of Figure 5a,b) resembles a diminishing of the diffraction maxima splitting indicating a decrease of the orthorhombic distortion. For the $x = 0.2$ composition, the structural change occurs at about 450 K which

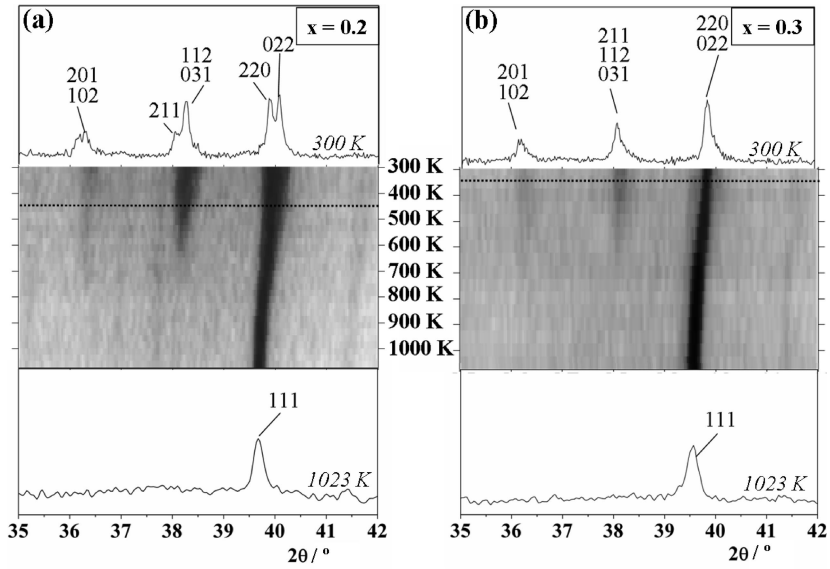

Figure 5. Temperature evolution of the XRD patterns for (a) $Na_{0.8}Sr_{0.1}NbO_3$ and (b) $Na_{0.7}Sr_{0.15}NbO_3$. Dashed lines indicate T_c for $Na_{0.8}Sr_{0.1}NbO_3$ and T_m for $Na_{0.7}Sr_{0.15}NbO_3$, respectively.

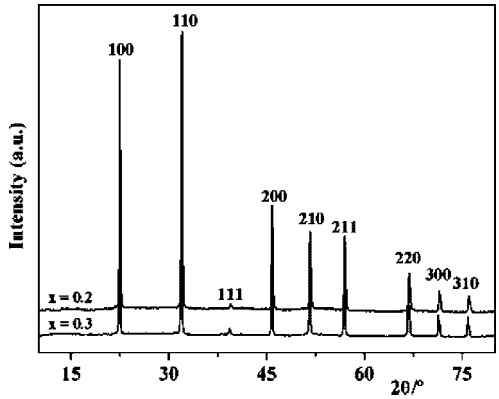

Figure 6. XRD pattern for $x = 0.2$ and $x = 0.3$ compositions recorded at 1023 K. Miller indices referred to a basic cubic perovskite cell.

could be correlated to the ferroelectric to paraelectric phase transition observed at $T_c = 448$ K. The structure becomes cubic around 650 K, where superstructure maxima cannot be observed (see lower part of Figure 5a). No structural phase transition across T_m (~344 K) is identified from the XRD data recorded as temperature increases for $x = 0.3$ (Figure 5b), which is in agreement with the observed relaxor behavior.[6] From 542 K, the material behaves as paraelectric (Figure 4e), although diffraction maxima corresponding to the orthorhombic cell are maintained up to ~650 K. From this temperature, the structure becomes cubic (see lower part of Figure 5b). Figure 6 displays the XRD patterns of the two samples recorded at 1023 K. For both compositions, all diffraction maxima could be indexed on the basis of a cubic unit cell.

The SAED pattern of a crystal of $Na_{0.6}Sr_{0.2}NbO_3$ is shown in Figure 7a. As in the $x = 0.3$ composition, the diffraction pattern can be interpreted as corresponding to the coexistence of structural domains of a $\sqrt{2}a_c \times 2a_c \times \sqrt{2}a_c$ unit cell oriented in the three perpendicular directions. Besides the (100) diffuse diffraction maxima (recall that this reflection appears by multiple diffraction), diffuse streaking along $[100]_c$ and $[010]_c$ reciprocal directions is visible. The corresponding high resolution micrograph shown in Figure 7b displays a heterogeneous contrast. In addition to the basic periodicity of 0.4 nm corresponding to the perovskite subcell, contrast which comprises two or three unit cells appears, doubling the $[100]_c$ and $[010]_c$ directions. The small orthorhombic distortion of this material is consistent with the observed contrast. A pseudocubic structure is formed as a consequence of the high A-vacancy concentration. Domains of the Q-like phase are not properly observed, and extra periodicities in respect to the basic perovskite can only be identified along several unit cells.

The temperature dependence of K' measured at different frequencies for the $x = 0.4$ composition is shown in Figure 8a. A broadened maximum is observed, the position of which is shifted to higher temperatures upon increasing the measuring frequency. It is worth mentioning that the frequency shift of T_m cannot be correctly fitted by the Vogel-Fulcher law, and unrealistic values of ω_0 with T_f below 0 K were obtained (Figure 8b). The fitting to an Arrhenius law (Figure 8c), despite it giving better fit, does not give a reliable value of ω_0, and this can be related to the rather small experimental frequency window available. Therefore, in spite of the frequency shift of T_m, this material does not behave as a canonical relaxor ferroelectric. In addition, very low remnant polarization (0.07 μC cm^{-2}) is found from the P versus E curve measured below T_m ($T = 80$ K; Figure 8d).

Discussion

The analysis of the room temperature XRD data of $Na_{1-x}Sr_{x/2}\square_{x/2}NbO_3$ indicates that samples over the composition range $0.2 \leq x \leq 0.4$ can be described considering an orthorhombically distorted perovskite type cell ($\sqrt{2}a_c \times 2a_c \times \sqrt{2}a_c$), although a clear reduction of the orthorhombic distortion is observed as strontium content increases (Figure 2b). Every introduced strontium atom generates one A-vacancy position to preserve the Nb(V) concentration. As stated from the transmission electron microscopy study, no evidence of extra strontium/sodium/vacancy order has been observed, indicating a random distribution of the vacancy

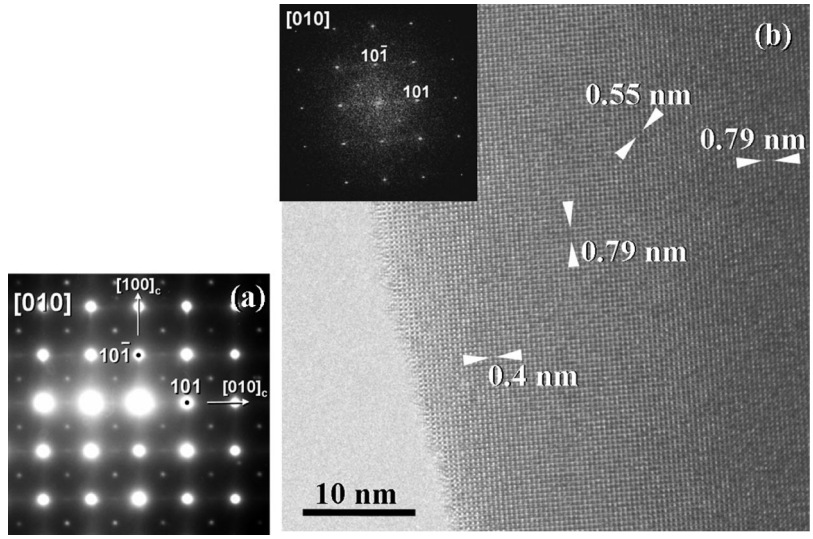

Figure 7. (a) SAED pattern of $Na_{0.6}Sr_{0.2}NbO_3$ taken along the [010] zone axis. Miller indices are referred to the $\sqrt{2}a_c \times 2a_c \times \sqrt{2}a_c$ unit cell. Diffuse streaking along the $[100]_c$ and $[010]_c$ reciprocal directions is observed. (b) Corresponding high resolution electron micrograph. Fourier transform is shown as inset.

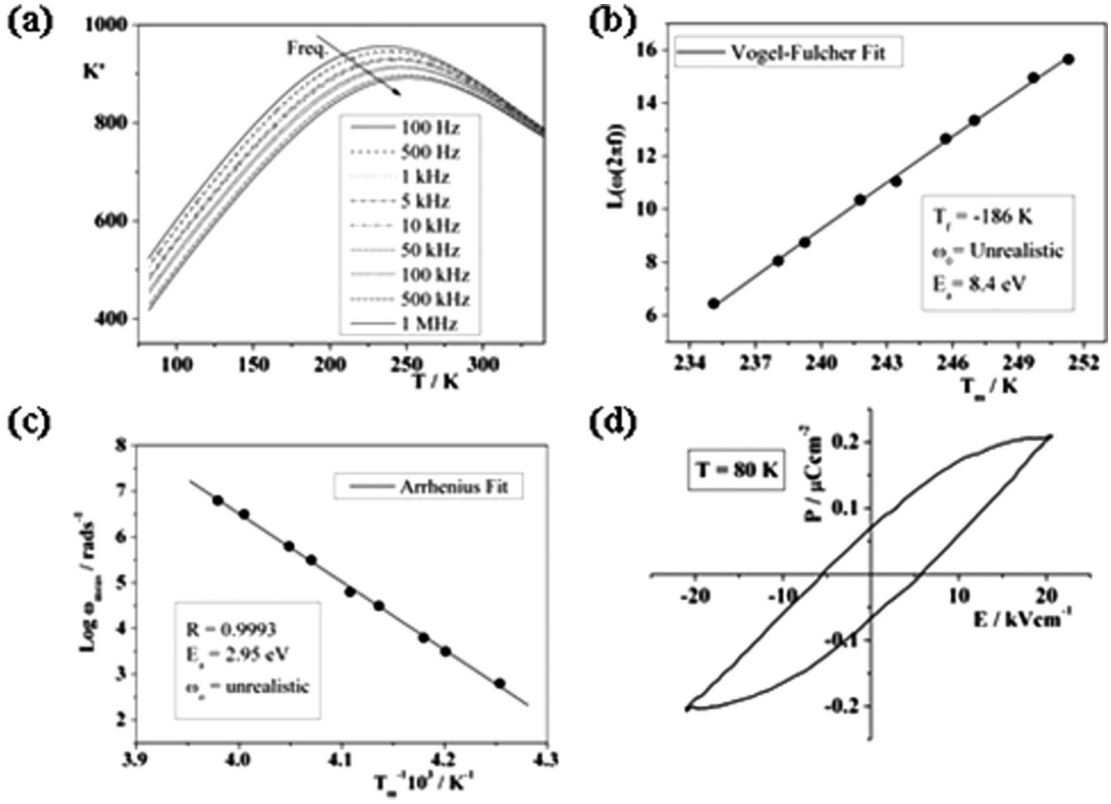

Figure 8. (a) Temperature dependence of K' at different measurement frequencies for $Na_{0.6}Sr_{0.2}NbO_3$. (b) The corresponding frequency dependence of T_m (points) cannot be fit by the Vogel-Fulcher relationship. (c) Frequency dependence of T_m (points) and Arrhenius fit. (d) Polarization vs Electric field curve at 80 K for the $Na_{0.6}Sr_{0.2}NbO_3$ material.

positions in the A sublattice of the perovskite structure. In addition, the increasing A-vacancy concentration progressively limits the growth of the structural coherent domains diminishing their average size.

The $Na_{0.7}Sr_{0.15}NbO_3$ material presents 15% of A-vacancy positions. From the electric characterization, relaxor-type behavior is observed for this composition. Following the generally accepted description, there are two essential conditions to the occurrence of relaxor ferroelectric behavior: (1) the existence of lattice disorder and (2) the presence of polar nanoregions (PNR) immersed on a nonpolar phase, which are responsible for the lost of the Curie−Weiss behavior of K' at temperatures higher than T_m.[6] For the $Na_{0.7}Sr_{0.15}NbO_3$ material, lattice disorder coming from the random distribution of the vacancy positions and sodium and strontium atoms in the A sublattice of the perovskite-type structure have been observed. On the other hand, the temperature dependence of $1/K'$ shows a strong deviation from the Curie−Weiss law from 542 K (Figure 4d), which indicates that the relaxor dynamics interaction of PNRs occurs at temperatures far above T_m (~344 K).

The structural characterization by TEM has revealed that the microstructure of the crystals at room temperature is constituted by structural nanodomains (~10 nm) which, from the observed contrast, can be assigned to the orthorhombic Q-like phase ($\sqrt{2}a_c \times 2a_c \times \sqrt{2}a_c$) intergrown in the three perpendicular directions. This microstructure can be compared with that of the $Na_{0.8}Sr_{0.10}NbO_3$ ferroelectric material although structural domains of the same unit cell metric appear 1 order of magnitude smaller.

Materials properties which depend on long-range order interactions might be influenced by the structural coherent domain grain size effect. Ferroelectric materials occur as a result of such a cooperative phenomenon, and the transformation to a relaxor ferroelectric implies the breakdown to a short-range order interaction. In this sense, several investigations on perovskite-type materials have analyzed the influence of the grain size on the appearance of diffuse phase transitions[28] and on the size induced relaxor properties.[29] A clear parallelism can be established between the decrease of the grain size leading to the procurement of relaxor ferroelectric materials and the growth limitation of the structural domains in $Na_{1-x}Sr_{x/2}\square_{x/2}NbO_3$ when increasing the A-vacancy concentration from the ferroelectric $x = 0.2$ to the relaxor ferroelectric $x = 0.3$ compositions. From the nanometric size of the structural domains observed in the relaxor material at room temperature (below T_f), one could assume a direct correspondence between the PNRs and the observed nanodomains. However, from the high temperature XRD study performed, we can state that the structure remains distorted above the temperature from which the material behaves as paraelectric ($T > 542$ K). The nonpolar phase, in contrast with the canonical relaxors, is a distorted noncubic perovskite type phase as shown by the presence of diffraction maxima at 36 and 38°/2θ. It indicates that the polar regions responsible for the relaxor character emerge in a structure phase which is already distorted, and therefore, the presence of PNRs should not be identified with the observed structural domains of nanometric size and they should not be larger than the observed structural domains.

The introduction of strontium and, therefore, A-vacancy positions in the material produces a chemical stress due to the expansive nature of the vacancy. In Figure 2b an increment on the cell volume is found on increasing the vacancy concentration that is coupled with a strong decrease of the orthorhombic distortion. The expansion of the cell can promote ferroelectric order as Raevski and Prosandeev found using the phenomenological Landau-type approach.[17] This approach can explain the change in nature from AFE $x = 0$ to FE $x = 0.2$ that we have previously reported.[20] Moreover, the local deformation around the defect can generate local dipolar moment which increases the dielectric dispersion in the material.[17] On the other hand the stress is known to affect the soft mode frequency and hence to reduce the correlation length, diminishing the possibility of long-range interactions.[6] In our case, the observed decrease in the coherent structural domain size can be related to the relief of the local mechanical stress produced by the vacancy though the formation of a larger quantity of domain walls. For $x = 0.3$ dipole formation must be now constrained to small clusters inside the average $\sqrt{2}a_c \times 2a_c \times \sqrt{2}a_c$ lattice, therefore avoiding the long-range dipole interaction of the ferroelectric state that occurs in the $x = 0.2$ composition. The relaxor ferroelectric character of the $x = 0.3$ material requires an applied electric field to reach the long-range ferroelectric interaction, and this is consistent with the disappearance of the ferroelectric to paraelectric transition observed for the $x = 0.2$ composition. The polarization (P) and electric field (E) measurements for $Na_{0.7}Sr_{0.15}NbO_3$ display hysteresis loops above T_m as shown in Figure 4c for selected temperatures. The $P(E)$ cycles become slimmer with increasing temperature, and the remnant polarization progressively decreases from T_f (see inset on Figure 4c). When exceeding T_m, the small P_r is an evidence of the presence of some degree of cooperative interaction of dipolar orientations.

In the $Na_{0.6}Sr_{0.2}NbO_3$ sample, 20% of A-vacancy positions are present. From the XRD data recorded at room temperature, the very low relative intensity of the superstructure diffraction maxima indicative of the orthorhombic symmetry (see inset on Figure 1c) suggests the material is pseudocubic, presenting a very small lattice distortion (Figure 2b). This is in agreement with the microstructure observed by TEM, where isolated areas restricted to a few unit cells show the contrast corresponding to the Q-like phase, the main contrast of the crystals corresponding to a pseudocubic lattice. In this sample the effect of the vacancy concentration is to further reduce the correlation length. In this sample, the relaxation observed in the dielectric constant by the introduction of 20% of A-vacancy positions provokes a lack of interaction between the polar moments which does not follow a Vogel-Fulcher relation; neither does it follow an Arrhenius behavior (Figure 8b,c). This change in the relaxation dynamics indicates the absence or strong decrease of correlations among the PNRs even at the lowest temperatures. The correlation between PNRs does not much increase by applying electric field as the doubtful hysteresis loop, Figure 8d, showed. The growing number of vacancies also produces a lowering in the values of the dielectric constant at the maximum, which goes from 1400 in $x = 0.3$ to 900 in $x = 0.4$.

From the data reported in the literature in sodium niobate-based relaxor solid solutions, the concentration dependence of the permittivity maximum temperature smoothly decays up to a certain x_0 value above which an abrupt drop takes place as well as the frequency dispersion of K'.[17−19] Our findings in the $Na_{1-x}Sr_{x/2}\square_{x/2}NbO_3$ system, however, show that a gradual and smooth decay of the permittivity maximum temperature occurs when increasing dopant concentration from $T_c = 633$ K for the pure sodium niobate[30] to $T_m = 240$ K for the $x = 0.4$ through $T_c = 543$ K,[20] $T_c = 448$ K, and $T_m = 344$ K for the $x = 0.1$, $x = 0.2$, and $x = 0.3$ compositions, respectively. The temperature at maximum of K' as a function of the Sr concentration between $x = 0$ and the limit of the solid solution $x = 0.4$, showed a linear behavior.

(28) Jo, W.; Kim, T.-H.; Kim, D.-Y.; Pabi, S. K. *J. Appl. Phys.* **2007**, *102*, 074116and references there in.
(29) Ziebert, C.; Schmitt, H.; Krüger, J. K.; Sternberg, A.; Ehses, K.-H. *Phys. Rev. B* **2004**, *69*, 214106.
(30) Landredi, S.; Rodrigues, A. C. M.; Dessemond, L. *J. Am. Ceram. Soc.* **2003**, *86*, 2103–2110.

Conclusions

The $Na_{0.7}Sr_{0.15}NbO_3$ material, which contains 15% of randomly distributed A-vacancy positions, displays ferroelectric relaxor character ($T_m = 344$ K at 1 kHz). The room temperature structural characterization performed shows the material retains the orthorhombically distorted Q-like phase structure previously observed for the ferroelectric $Na_{0.8}Sr_{0.1}NbO_3$. Transmission electron microscopy reveals a complex microstructure constituted by structural nanodomains of the orthorhombic Q-like phase, which must be a direct consequence of the high A-vacancy concentration. The observed decrease in the coherent structural domain size can be related to relieving the local mechanical stress produced by the vacancy through the formation of a larger quantity of domain walls. It generates the breaking of the long coherent length of the polar domains responsible for the ferroelectric relaxor behavior. The high temperature X-ray diffraction study performed indicates that the structure remains distorted above the temperature from which the material behaves as paraelectric ($T > 542$ K), and therefore, a direct correlation between regions of polar phase and the nanostructured observed domains cannot be established. It indicates that the polar regions responsible for the relaxor character emerge in an already distorted structure phase with the same metric as the polar phase.

When increasing dopant content to generate 20% of A-vacancy positions, the $Na_{0.6}Sr_{0.2}NbO_3$ material shows a change in the relaxation dynamics. The material presents a very small orthorhombic lattice distortion, and the microstructure observed by TEM reveals isolated areas restricted to a few unit cells, showing the contrast corresponding to the Q-like phase. The effect of the high vacancy concentration is to further reduce the correlation length, showing the absence or strong decrease of correlations among the polar regions even at the lowest temperatures.

The modification of the dielectric properties in the $Na_{1-x}Sr_{x/2}\square_{x/2}NbO_3$ system ($0.3 \leq x \leq 0.4$) occurs through the doping process as a consequence of an increasing amount of randomly distributed A-vacancy positions. Cationic vacancies limit dipole formation to small clusters inside the average $\sqrt{2}a_c \times 2a_c \times \sqrt{2}a_c$ lattice, therefore avoiding the long-range dipole interaction.

Acknowledgment. Financial support from DGICYT in Spain through Projects MAT2007-61954 and MAT2007-61409 is gratefully acknowledged. Authors are grateful to the Centro de Difracción de Rayos X (U.C.M.) and to the Centro de Microscopia Electrónica (U.C.M.) for facilities.

CM9000834